

ISSN: 0256-307X

# 中国物理快报 Chinese Physics Letters

Volume 27 Number 5 May 2010

A Series Journal of the Chinese Physical Society  
Distributed by IOP Publishing

Online: <http://www.iop.org/journals/cpl>  
<http://cpl.iphy.ac.cn>

CHINESE PHYSICAL SOCIETY

JUST FOR AUTHORS  
— CHINESE PHYSICS LETTERS

## Neutron Spectroscopic Factors of ${}^7\text{Li}$ and Astrophysical ${}^6\text{Li}(n,\gamma){}^7\text{Li}$ Reaction Rates \*

SU Jun(苏俊)\*\*, LI Zhi-Hong(李志宏), GUO Bing(郭冰), BAI Xi-Xiang(白希祥), LI Zhi-Chang(李志常),  
LIU Jian-Cheng(刘建成), WANG You-Bao(王友宝), LIAN Gang(连钢), ZENG Sheng(曾晟),  
WANG Bao-Xiang(王宝祥), YAN Sheng-Quan(颜胜权), LI Yun-Ju(李云居), LI Er-Tao(李二涛),  
FAN Qi-Wen(樊启文), LIU Wei-Ping(柳卫平)

China Institute of Atomic Energy, PO Box 275(10), Beijing 102413

(Received 22 October 2009)

Angular distributions of the  ${}^7\text{Li}({}^6\text{Li}, {}^6\text{Li}){}^7\text{Li}$  elastic scattering and the  ${}^7\text{Li}({}^6\text{Li}, {}^7\text{Li}_{\text{g.s.}}){}^6\text{Li}$ ,  ${}^7\text{Li}({}^6\text{Li}, {}^7\text{Li}_{0.48}){}^6\text{Li}$  transfer reactions at  $E_{\text{c.m.}} = 23.7$  MeV are measured with the Q3D magnetic spectrograph. The optical potential of  ${}^6\text{Li} + {}^7\text{Li}$  is obtained by fitting the elastic scattering differential cross sections. Based on the distorted wave Born approximation (DWBA) analysis, spectroscopic factors of  ${}^7\text{Li} = {}^6\text{Li} \otimes n$  are determined to be  $0.73 \pm 0.05$  and  $0.90 \pm 0.09$  for the ground and first excited states in  ${}^7\text{Li}$ , respectively. Using the spectroscopic factors, the cross sections of the  ${}^6\text{Li}(n, \gamma_0, 1){}^7\text{Li}$  direct neutron capture reactions and the astrophysical  ${}^6\text{Li}(n, \gamma){}^7\text{Li}$  reaction rates are derived.

PACS: 21.10.Jx, 25.60.Bx, 25.60.Je, 26.35.+c

DOI: 10.1088/0256-307X/27/5/052101

Recently, lithium isotopes have attracted an intense interest because the abundance of both  ${}^6\text{Li}$  and  ${}^7\text{Li}$  from big bang nucleosynthesis (BBN) is one of the puzzles in nuclear astrophysics. According to the baryon density determined by the Wilkinson microwave anisotropy probe (WMAP),<sup>[1]</sup> the primary abundances for  ${}^6\text{Li}$  and  ${}^7\text{Li}$  predicted by the standard BBN (SBBN) model deviate clearly from the observations of the metal-poor halo stars,<sup>[2]</sup> where the lithium abundances exhibit a “plateau” behavior.<sup>[3]</sup> Several investigations for both astrophysical observation and nucleosynthesis calculation have been attempted to explain the large discrepancies, but none of them has been successful up to now. In addition, due to the difference between the depletion speeds of  ${}^6\text{Li}$  and  ${}^7\text{Li}$  in stars, the  ${}^6\text{Li}/{}^7\text{Li}$  ratio could stand for a measure of the time scale for stellar evolution. In the above scenario,  ${}^6\text{Li}(n, \gamma){}^7\text{Li}$  is believed to be one of the important reactions in the SBBN network,<sup>[4,5]</sup> its reaction rates would affect the abundances of both  ${}^6\text{Li}$  and  ${}^7\text{Li}$ .

The cross sections of  ${}^6\text{Li}(n, \gamma){}^7\text{Li}$  at astrophysically relevant energies are most likely dominated by the E1 transitions into the ground and the first excited states in  ${}^7\text{Li}$ . To date, only one direct measurement of the  ${}^6\text{Li}(n, \gamma){}^7\text{Li}$  cross sections with three data points at stellar energies has been performed.<sup>[6]</sup> The cross sections of direct radiative capture reaction can also be calculated by the direct capture model with the spectroscopic information extracted from the single particle transfer reaction.<sup>[7–10]</sup> In previous studies, the spectroscopic factors were mostly derived

by  ${}^6\text{Li}(d, p){}^7\text{Li}$  and  ${}^7\text{Li}(p, d){}^6\text{Li}$  reactions,<sup>[11–15]</sup> the results are correlative with the neutron spectroscopic factor of deuteron. Thus, it is highly desired to extract the spectroscopic factors through a self-contained reaction without a third-participant, which can provide an independent verification.

The elastic-transfer reaction is a good tool for extracting the single nucleon spectroscopic factors, which have been used to determine the spectroscopic factor of  ${}^9\text{Be} = {}^8\text{Li} \otimes p$  with the  ${}^9\text{Be}({}^8\text{Li}, {}^9\text{Be}){}^8\text{Li}$  reaction.<sup>[16]</sup> In such an approach, the events from elastic scattering and elastic-transfer reaction can not be distinguished, but the theoretical calculation shows that their mutual contributions at the respective forward angles are negligibly small. As a result, the effective differential cross sections at forward angles of the two processes can be obtained, respectively. The obvious advantages of this approach are (i) the elastic scattering and elastic-transfer reaction have the same entrance and exit channels, the spectroscopic factor can be derived by one set of optical potential deduced from the elastic scattering and (ii) the elastic-transfer reaction does not involve third participant in the entrance and exit channels, and thus results in a reduction of experimental result uncertainty.

For the above reasons, we choose the  ${}^7\text{Li}({}^6\text{Li}, {}^7\text{Li}){}^6\text{Li}$  elastic-transfer reaction to extract the spectroscopic factors of the  ${}^7\text{Li} = {}^6\text{Li} \otimes n$ . This reaction has been measured in 1998 at  $E_{\text{lab}} = 9\text{--}40$  MeV,<sup>[17]</sup> unfortunately the minimum angle reached in that experiment is about  $30^\circ$  in the center of mass frame (for transfer process), which is not

\*Supported by the National Basic Research Program of China under Grant No 2007CB815003, the National Natural Science Foundation of China under Grant Nos 10675173, 10720101076, 10735100 and 10975193.

\*\*Email: junsu@ciae.ac.cn

© 2010 Chinese Physical Society and IOP Publishing Ltd

suitable to derive the spectroscopic factor. In the present work, we measure the angular distributions of the  ${}^7\text{Li}({}^6\text{Li}, {}^6\text{Li}){}^7\text{Li}$  elastic scattering and  ${}^7\text{Li}({}^6\text{Li}, {}^7\text{Li}_{\text{g.s.}}){}^6\text{Li}$ ,  ${}^7\text{Li}({}^6\text{Li}, {}^7\text{Li}_{0.48}){}^6\text{Li}$  transfer reactions at  $E_{\text{c.m.}} = 23.7$  MeV. The neutron spectroscopic factors for the ground and first excited states in  ${}^7\text{Li}$  are determined by comparing the experimental results with the distorted-wave Born approximation (DWBA) calculations, and then used to calculate the cross sections and astrophysical rates of  ${}^6\text{Li}(n, \gamma){}^7\text{Li}$  direct capture reaction.

The experiment was carried out at the Beijing HI-13 tandem accelerator. A 44 MeV  ${}^6\text{Li}$  beam with an intensity of about 100 pA impinged on the natural LiF target with a thickness of  $530 \mu\text{g}/\text{cm}^2$ , which is evaporated on a  $50 \mu\text{g}/\text{cm}^2$  carbon foil. The beam was collected by a Faraday cup behind the target for counting the number of  ${}^6\text{Li}$ . The Faraday cup covered an angular range of  $\pm 6^\circ$  and confined the attainable minimum angle in the measurement. The reaction products were focused and separated by Q3D magnetic spectrograph. The accepted solid angle of Q3D was set to be 0.23 mSr for a good angular resolution. A two-dimensional position sensitive silicon detector (PSSD) was set at the focal plane of Q3D, the  $X - Y$  information from PSSD enabled the products emitted into the accepted solid angle of Q3D to be fully recorded, and the corresponding energy signals were used to remove the impurities with the same magnetic rigidity. The absolute differential cross sections were determined by normalizing the measurements of the  ${}^7\text{Li}({}^6\text{Li}, {}^6\text{Li}){}^7\text{Li}$  elastic scattering and the  ${}^7\text{Li}({}^6\text{Li}, {}^7\text{Li}_{\text{g.s.}}){}^6\text{Li}$ ,  ${}^7\text{Li}({}^6\text{Li}, {}^7\text{Li}_{0.48}){}^6\text{Li}$  transfer reactions to the elastic scattering of  ${}^6\text{Li}$  on the gold target at  $\theta_{\text{lab}} = 25^\circ$ .

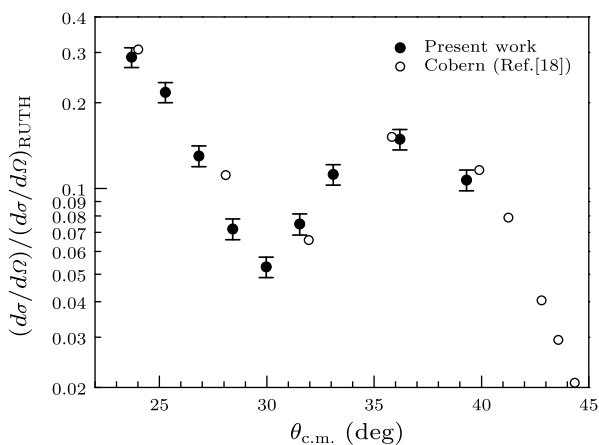


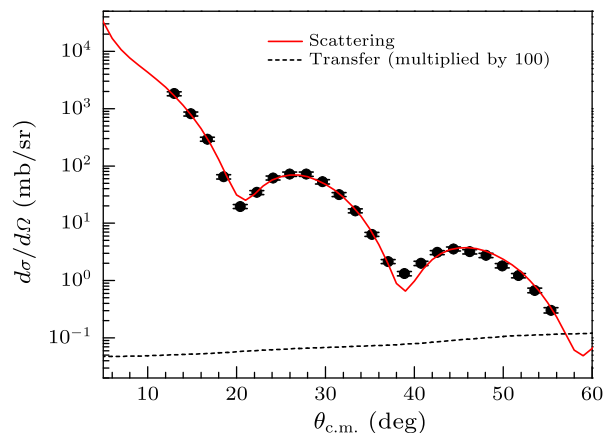
**Fig. 1.** Comparison of the  ${}^{12}\text{C}({}^7\text{Li}, {}^7\text{Li}){}^{12}\text{C}$  angular distributions at  $E_{\text{lab}} = 36$  MeV, the solid and open circles denote the data obtained in the present experiment and in an earlier work,<sup>[18]</sup> respectively.

The experimental setup was tested beforehand by measuring the angular distribution of  ${}^{12}\text{C}({}^7\text{Li}, {}^7\text{Li}){}^{12}\text{C}$

elastic scattering at  $E_{\text{lab}} = 36$  MeV. As shown in Fig. 1, our result is in fair agreement with that reported in Ref. [18], indicating a reliable overall performance of our setup and data analysis procedure.

In the measurements of  ${}^7\text{Li}({}^6\text{Li}, {}^6\text{Li}){}^7\text{Li}$  elastic scattering and  ${}^7\text{Li}({}^6\text{Li}, {}^7\text{Li}_{\text{g.s.}}){}^6\text{Li}$ ,  ${}^7\text{Li}({}^6\text{Li}, {}^7\text{Li}_{0.48}){}^6\text{Li}$  transfer reactions, the magnetic fields of Q3D were set to focus  ${}^6\text{Li}$  and  ${}^7\text{Li}$ , respectively. The elastic scattering and transfer processes were measured in the angular ranges of  $7^\circ \leq \theta_{\text{lab}} \leq 30^\circ$  and  $7^\circ \leq \theta_{\text{lab}} \leq 17^\circ$  in steps of  $1^\circ$ , respectively.

The differential cross sections for elastic scattering are shown in Fig. 2, with uncertainties from the errors of statistics and target thickness. The angular distribution of  ${}^7\text{Li}({}^6\text{Li}, {}^6\text{Li}){}^7\text{Li}$  elastic scattering was analyzed by employing the code PTOLEMY<sup>[19]</sup> and optical model using real and imaginary potentials with Woods-Saxon form. The optimized potential parameters obtained by fitting the experimental data are listed in Table 1. The fitting results are shown in Fig. 2 together with the experimental data. Figure 2 also exhibits the contribution of transfer processes, which is less than 1% within the experimental angular range.



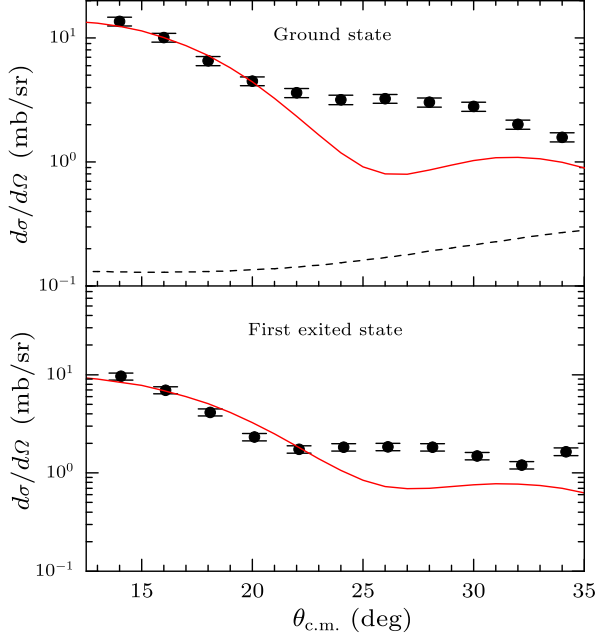
**Fig. 2.** Differential cross sections for  ${}^7\text{Li}({}^6\text{Li}, {}^6\text{Li}){}^7\text{Li}$  elastic scattering at  $E_{\text{c.m.}} = 23.7$  MeV together with the optical model calculation. The dashed line denotes the contribution of transfer processes (multiplied by a factor of 100).

Table 1. Optical potential parameters for  ${}^6\text{Li} + {}^7\text{Li}$  system at  $E_{\text{c.m.}} = 23.7$  MeV. The depths and geometrical parameters are in MeV and fm, respectively.

$U_V$	$r_R$	$a_R$	$W_V$	$r_I$	$a_I$	$r_c$	$\chi^2/\text{point}$
73.4	0.5	0.92	32.6	1.0	0.8	1.25	4.0

The angular distributions of  ${}^7\text{Li}({}^6\text{Li}, {}^7\text{Li}_{\text{g.s.}}){}^6\text{Li}$  and  ${}^7\text{Li}({}^6\text{Li}, {}^7\text{Li}_{0.48}){}^6\text{Li}$  transfer processes are shown in Fig. 3, which are also analyzed with the code PTOLEMY. As can clearly be seen from Fig. 3, the contribution of elastic scattering is very small. In the calculation, we utilize the  ${}^6\text{Li} + {}^7\text{Li}$  optical potential parameters listed in Table 1 for both the entrance and

exit channels. For the bound states, a Woods–Saxon potential with the standard geometrical parameters  $r_0 = 1.25$  fm and  $a = 0.65$  fm is adopted and the depths are adjusted to reproduce the neutron binding energies of  ${}^7\text{Li}$ .



**Fig. 3.** Angular distribution of  ${}^7\text{Li}({}^6\text{Li}, {}^7\text{Li}_{\text{g.s.}}){}^6\text{Li}$  and  ${}^7\text{Li}({}^6\text{Li}, {}^7\text{Li}_{0.48}){}^6\text{Li}$  at  $E_{\text{c.m.}} = 23.7$  MeV together with the DWBA calculations normalized to the first three data at forward angles. The dashed line denotes the contribution of elastic scattering (multiplied by a factor of 1000).

The spectroscopic factor  ${}^7\text{Li} = {}^6\text{Li} \otimes n$ , denoted as  $S_{7\text{Li}}$ , can be derived by normalizing the DWBA calculations to the experimental data according to the expression

$$\left(\frac{d\sigma}{d\Omega}\right)_{\text{EXP}} = S_{7\text{Li}}^2 \left(\frac{d\sigma}{d\Omega}\right)_{\text{DWBA}}. \quad (1)$$

Generally, the experimental data in the first peak of angular distributions at the forward angles are suitable for extracting the spectroscopic factor<sup>[20]</sup> because the differential cross sections of other angles are more sensitive to some high-order processes. In our calculation, only the first three data at the forward angles were used to extract the spectroscopic factors. For the  ${}^7\text{Li}({}^6\text{Li}, {}^7\text{Li}_{\text{g.s.}}){}^6\text{Li}$  channel, both of the neutron transfers to the  $1p_{3/2}$  and  $1p_{1/2}$  orbits of  ${}^7\text{Li}$  were taken into account, consequently the result was the coherent sum of their contributions. Since the  $1p_{3/2}$  and  $1p_{1/2}$  components can not be distinguished experimentally, their ratio was taken to be 1.5 based on the calculation,<sup>[21]</sup> then the spectroscopic factor of  ${}^7\text{Li}_{\text{g.s.}} = {}^6\text{Li} \otimes n$  was determined to be  $0.73 \pm 0.05$ , the uncertainty results from the measurement, scattering potential fitting and the divergence of the values derived from three different angles. For the first excited

state in  ${}^7\text{Li}$ , only the neutron transfer to the  $1p_{3/2}$  orbit was considered because the contribution of  $1p_{1/2}$  orbit is merely about 4%,<sup>[21]</sup> then the spectroscopic factor of  ${}^7\text{Li}_{0.48} = {}^6\text{Li} \otimes n$  is derived to be  $0.90 \pm 0.09$ . The spectroscopic factors obtained in several theoretical and experimental investigations are listed in Table 2, our results agree well with the theoretical calculation<sup>[21–24]</sup> and the experimental data.<sup>[12,13]</sup>

Table 2. Theoretical and experimental neutron spectroscopic factors for the ground and first excited states in  ${}^7\text{Li}$ .

$S_{7\text{Li}_{\text{g.s.}}}$	$S_{7\text{Li}_{0.48}}$	Experiments or theory	Reference
0.72	0.89	Theory	[21]
0.80	0.98	Theory	[22]
0.79	0.97	theory	[23]
0.77	1.07	Theory	[24]
0.90	1.15	${}^6\text{Li}(d, p)$	[11]
0.71		${}^7\text{Li}(p, d)$	[12]
$0.72 \pm 0.1$		${}^7\text{Li}(p, d)$	[13]
0.87		${}^7\text{Li}(p, d)$	[14]
$1.85 \pm 0.37$		${}^6\text{Li}(d, p)$	[15]
$0.73 \pm 0.05$	$0.90 \pm 0.09$	${}^7\text{Li}({}^6\text{Li}, {}^7\text{Li})$	Present work

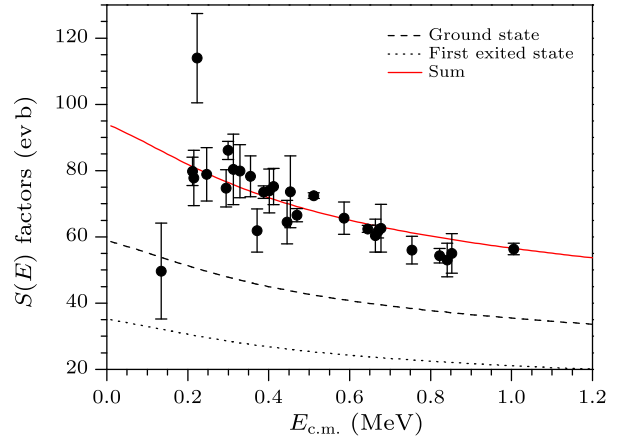


**Fig. 4.** Astrophysical  $S(E)$  factors of the  ${}^6\text{Li}(p, \gamma){}^7\text{Be}$  reaction. The experimental data are taken from Ref. [26].

At low energies of astrophysical interest, the  ${}^6\text{Li}(n, \gamma){}^7\text{Li}$  direct capture cross sections are dominated by the E1 transition from incoming s-wave to the bound state, the contribution of d-wave neutrons is negligible. In the computation we used the code RADCAP<sup>[25]</sup> and Woods–Saxon form potential with the standard geometrical parameters. The potential depths of the  ${}^7\text{Li}$  bound states are adjusted to reproduce the neutron binding energies of its ground and first excited states, respectively. For the scattering potential, the depth can be fixed by fitting the well measured  ${}^6\text{Li}(p, \gamma){}^7\text{Be}$  cross sections at low energies<sup>[26]</sup> because the difference between  $n+{}^6\text{Li}$  and  $p+{}^6\text{Li}$  potentials is only a Coulomb modification of depth, which is given by  $\Delta V = 0.4Z/A^{1/3}$ .<sup>[27]</sup>

The  ${}^6\text{Li}(p, \gamma){}^7\text{Be}$  cross sections are also calculated by the same code. The neutron spectroscopic factors of  ${}^7\text{Li}$  derived above are correspondingly taken as the proton spectroscopic factors for the ground and first

exited states in  ${}^7\text{Be}$  owing to the charge symmetry. Here the depth of scattering potential is constrained to be  $41.3 \pm 2.0$  MeV in reproducing the experimental data. The calculated astrophysical  ${}^6\text{Li}(p, \gamma){}^7\text{Be}$   $S(E)$  factors are shown in Fig. 4 together with the experimental results. In addition to a good agreement between the calculated and measured total  $S(E)$  factors, our calculation also indicates that the contributions of ground and first excited states are about 63% and 37%, respectively, which are very close to the experimental values 61% and 39%.<sup>[27]</sup>

Considering the Coulomb modification, the scattering potential depth of  $n + {}^6\text{Li}$  is chosen to be  $40.6 \pm 2.0$  MeV. Then the  ${}^6\text{Li}(n, \gamma){}^7\text{Li}_{\text{g.s.}}$  and  ${}^6\text{Li}(n, \gamma){}^7\text{Li}_{0.48}$  cross sections are calculated using the spectroscopic factors and optical potentials extracted above, and compared with the experimental data,<sup>[6]</sup> as shown in Fig. 5. Our result is consistent with the direct measurement, showing an approximate  $1/v$  behavior, so that the reaction rates are almost constant at energies of astrophysical interest.

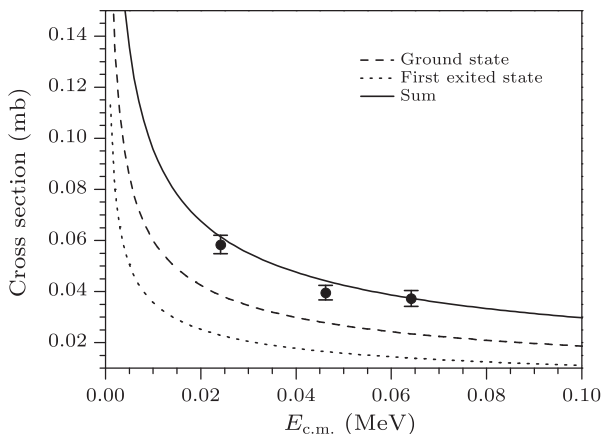


**Fig. 5.** Cross sections of the  ${}^6\text{Li}(n, \gamma){}^7\text{Li}$  reaction. The experimental data are taken from Ref. [6].

The astrophysical  ${}^6\text{Li}(n, \gamma){}^7\text{Li}$  direct capture reaction rate is then calculated by the expression<sup>[25]</sup>

$$N_A \langle \sigma v \rangle = 3.73 \times 10^{10} A^{-\frac{1}{2}} T_9^{-\frac{3}{2}} \times \int_0^\infty \sigma E \exp\left(-\frac{11.6E}{T_9}\right) dE, \quad (2)$$

where  $A$  is the reduced mass in atomic unit,  $T_9$  is the temperature in units of  $10^9$  K.  $E$ ,  $\sigma$  and reaction rate are given in MeV, barns and  $\text{cm}^3\text{mol}^{-1}\text{s}^{-1}$ , respectively. The reaction rate is found to be  $(8.5 \pm$

$1.7) \times 10^3 \text{ cm}^3\text{mol}^{-1}\text{s}^{-1}$ , with the error resulted from the uncertainties of spectroscopic factors and scattering potential depth.

In summary, the measurements of differential cross sections for the  ${}^7\text{Li}({}^6\text{Li}, {}^6\text{Li}){}^7\text{Li}$  elastic scattering and  ${}^7\text{Li}({}^6\text{Li}, {}^7\text{Li}_{\text{g.s.}}){}^6\text{Li}$ ,  ${}^7\text{Li}({}^6\text{Li}, {}^7\text{Li}_{0.48}){}^6\text{Li}$  transfer reactions have been carried out at  $E_{\text{c.m.}} = 23.7$  MeV, in which the angular distributions for transfer processes are obtained in the range of  $14^\circ \lesssim \theta_{\text{c.m.}} \lesssim 34^\circ$  for the first time. By using the optical potential of  ${}^6\text{Li} + {}^7\text{Li}$  extracted from the elastic scattering, the spectroscopic factors of  ${}^7\text{Li} = {}^6\text{Li} \otimes n$  are deduced with the DWBA analysis, the results are in agreement with those reported previously.<sup>[12,13,21–24]</sup> Then the  ${}^6\text{Li}(n, \gamma){}^7\text{Li}$  direct capture cross sections have been derived and compared with the direct measurement data. The astrophysical reaction rate is found to be higher by a factor of 1.7 than the value adopted in previous reaction network calculations.<sup>[4,5]</sup>

## References

- [1] Dunkley J et al 2009 *Astrophys. J. Suppl.* **180** 306
- [2] Cayrel R et al 2008 arXiv:0810.4290v2
- [3] Spite F and Spite M 1982 *Astron. Astrophys.* **115** 357
- [4] Malaney R A and Fowler W A 1989 *Astrophys. J.* **345** L5
- [5] Nollett K M, Lemoine M and Schramm D N 1997 *Phys. Rev. C* **56** 1144
- [6] Toshiro O et al 2000 *AIP Conference Proceedings* **529** 678
- [7] Li Z H et al 2005 *Phys. Rev. C* **71** 052801(R)
- [8] Su J et al 2006 *Chin. Phys. Lett.* **23** 55
- [9] Li Z H et al 2006 *Phys. Rev. C* **74** 035801
- [10] Guo B et al 2007 *Chin. Phys. Lett.* **24** 65
- [11] Schiffer J P et al 1967 *Phys. Rev.* **164** 1274
- [12] Li T Y and Mark S K 1969 *Nucl. Phys. A* **123** 147
- [13] Towner I S 1969 *Nucl. Phys. A* **126** 97
- [14] Fagerström B et al 1976 *Physica Scripta* **13** 101
- [15] Tsang M B, Lee J and Lynch W G 2005 *Phys. Rev. Lett.* **95** 222501
- [16] Camargo O et al 2008 *Phys. Rev. C* **78** 034605
- [17] Potthast K W et al 1998 *Nucl. Phys. A* **629** 656
- [18] Cobern M E, Pisano D J and Parker P D 1976 *Phys. Rev. C* **14** 491
- [19] Macfarlane M H and Pieper S C 1976 *Argonne Nat. Lab. Report No ANL-76-11* (unpublished)
- [20] Liu X D et al 2004 *Phys. Rev. C* **69** 064313
- [21] Cohen S and Kurath D 1967 *Nucl. Phys. A* **101** 1
- [22] Barker F C 1966 *Nucl. Phys. A* **83** 418
- [23] Varma S and Goldhammer P 1969 *Nucl. Phys. A* **125** 193
- [24] Kumar N 1974 *Nucl. Phys. A* **225** 221
- [25] Bertulani C A 2003 *Comput. Phys. Commun.* **156** 123
- [26] Switkowski Z E et al 1979 *Nucl. Phys. A* **331** 50
- [27] Dave J H and Gould C R 1983 *Phys. Rev. C* **28** 2212
- [28] Angulo C 1999 *Nucl. Phys. A* **656** 3

# Chinese Physics Letters

Volume 27

Number 5

2010

## GENERAL

- 050201 The Multi-Function Jaulent–Miodek Equation Hierarchy with Self-Consistent Sources**  
YU Fa-Jun
- 050301 A New Kind of Integration Transformation in Phase Space Related to Two Mutually Conjugate Entangled-State Representations and Its Uses in Weyl Ordering of Operators**  
LV Cui-Hong, FAN Hong-Yi
- 050302 Evolution of Number State to Density Operator of Binomial Distribution in the Amplitude Dissipative Channel**  
FAN Hong-Yi, REN Gang
- 050303 Evolutionarily Stable Strategies in Quantum Hawk–Dove Game**  
Ahmad Nawaz, A. H. Toor
- 050304 Fidelity Susceptibility in the SU(2) and SU(1,1) Algebraic Structure Models**  
ZHANG Hong-Biao, TIAN Li-Jun
- 050305 Squeezing-Displacement Dynamics for One-Dimensional Potential Well with Two Mobile Walls where Wavefunctions Vanish**  
FAN Hong-Yi, CHEN Jun-Hua, WANG Tong-Tong
- 050306 A New Quantum Secure Direct Communication Scheme with Authentication**  
LIU Dan, PEI Chang-Xing, QUAN Dong-Xiao, ZHAO Nan
- 050401 Mechanical and Thermal Properties of the AH of FRW Universe**  
WEI Yi-Huan
- 050501 Chaotic Dynamics of a Josephson Junction with Nonlinear Damping**  
LI Fei, PAN Chang-Ning, ZHANG Dong-Xia, TANG Li-Qiang
- 050502 Adaptive Function Projective Synchronization of Discrete Chaotic Systems with Unknown Parameters**  
WU Zhao-Yan, FU Xin-Chu
- 050503 Cluster Consensus of Nonlinearly Coupled Multi-Agent Systems in Directed Graphs**  
LU Xiao-Qing, Francis Austin, CHEN Shi-Hua
- 050601 Determination of Mean Thickness of an Oxide Layer on a Silicon Sphere by Spectroscopic Ellipsometry**  
ZHANG Ji-Tao, LI Yan, LUO Zhi-Yong, WU Xue-Jian
- 050701 Preparation and Humidity Sensing Properties of KCl/MCM-41 Composite**  
LIU Li, KOU Li-Ying, ZHONG Zhi-Cheng, WANG Lian-Yuan, LIU Li-Fang, LI Wei

## THE PHYSICS OF ELEMENTARY PARTICLES AND FIELDS

- 051101 Prospects on Determining Electric Dipole Moments of  $\Sigma$  and  $\Xi$  Hyperons at BESIII**  
ZHANG Feng, GAO Yuan-Ning, HUO Lei
- 051301  $B_s$  Semileptonic Decays to  $D_s$  and  $D_s^*$  in Bethe–Salpeter Method**  
ZHANG Jin-Mei, WANG Guo-Li

## NUCLEAR PHYSICS

- 052101 Neutron Spectroscopic Factors of  ${}^7\text{Li}$  and Astrophysical  ${}^6\text{Li}(n,\gamma){}^7\text{Li}$  Reaction Rates**  
SU Jun, LI Zhi-Hong, GUO Bing, BAI Xi-Xiang, LI Zhi-Chang, LIU Jian-Cheng, WANG You-Bao, LIAN Gang, ZENG Sheng, WANG Bao-Xiang, YAN Sheng-Quan, LI Yun-Ju, LI Er-Tao, FAN Qi-Wen, LIU Wei-Ping

(Continued on inside back cover)

- 052501 Emission of Neutral Pions with High Transverse Momenta in A-A and p-p Collisions at Energies Available at the BNL Relativistic Heavy Ion Collider**  
FAN San-Hong, MENG Cai-Rong, LIU Fu-Hu
- 052502 Influence of the Nucleon Hard Partons Distribution on  $J/\Psi$  Suppression in a GMC Framework**  
WANG Hong-Min, HOU Zhao-Yu, SUN Xian-Jing
- 052503 Rapidity Losses in Heavy-Ion cCollisions from AGS to RHIC Energies**  
ZHOU Feng-Chu, YIN Zhong-Bao, ZHOU Dai-Cui
- 052901 Gallium Nitride Room Temperature  $\alpha$  Particle Detectors**  
LU Min, ZHANG Guo-Guang, FU Kai, YU Guo-Hao
- 052902 Optimization of Experimental Discharge Parameters to Increase the Arc Efficiency of the Bucket Ion Source**  
YU Li-Ming, LEI Guang-Jiu, CAO Jian-Yong, ZHONG Guang-Wu, JIANG Shao-Feng, ZOU Gui-Qing, JIANG Tao, LU Da-Lun, ZHANG Xian-Ming, LIU He
- 052903 Varying Track Etch Rates along the Fission Fragments' Trajectories in CR-39 Detectors**  
N. Ali, E. U. Khan, A. Waheed, S. Karim, F. Khan, A. Majeed

#### **ATOMIC AND MOLECULAR PHYSICS**

- 053201 Chip-Based Square Wave Dynamic Micro Atom Trap**  
DAN Lin, YAN Hui, WANG Jin, ZHAN Ming-Sheng
- 053202 A Novel Observation of "a Sharp Absorption Line" Using Much More Broad Laser Lights: Quantum Interference in the Autoionization Spectra of Sc**  
ZHONG Zhi-Ping, GAO Xiang, ZHANG Xiao-Le, LI Jia-Ming
- 053401 Collision of Low Energy Proton with Ethylene**  
WANG Zhi-Ping, WANG Jing, ZHANG Feng-Shou
- 053701 Ionization Detection of Ultracold Ground State Cesium Molecules**  
JI Zhong-Hua, WU Ji-Zhou, MA Jie, FENG Zhi-Gang, ZHANG Lin-Jie, ZHAO Yan-Ting, WANG Li-Rong, XIAO Lian-Tuan, JIA Suo-Tang

#### **FUNDAMENTAL AREAS OF PHENOMENOLOGY(INCLUDING APPLICATIONS)**

- 054101 Rayleigh Scattering for An Electromagnetic Anisotropic Medium Sphere**  
LI Ying-Le, WANG Ming-Jun, DONG Qun-Feng, TANG Gao-Feng
- 054201 Characteristics and New Measurement Method of NCSFs of Individual Color Mechanisms of Human Vision**  
GE Jing-Jing, WANG Zhao-Qi, WANG Yan, ZHAO Kan-Xing
- 054202 A Phase-Controlled Optical Parametric Amplifier Pumped by Two Phase-Distorted Laser Beams**  
REN Hong-Yan, QIAN Lie-Jia, YUAN Peng, ZHU He-Yuan, FAN Dian-Yuan
- 054203 Broadband Convergence of 40 GHz-ROF and 10-Gb/s WDM-PON Systems in the Duplex Access Network**  
ZHANG Li-Jia, XIN Xiang-Jun, LIU Bo, ZHANG Qi, WANG Yong-Jun, YU Chong-Xiu
- 054204 Fabrication and Characterization of High Power InGaN Blue-Violet Lasers with an Array Structure**  
JI Lian, ZHANG Shu-Ming, JIANG De-Sheng, LIU Zong-Shun, ZHANG Li-Qun, ZHU Jian-Jun, ZHAO De-Gang, DUAN Li-Hong, YANG Hui
- 054205 A Hybrid Method of Solving the Electromagnetic Inverse Scattering Problem in Lossy Medium**  
YANG Xi, ZHANG Yu, GOU Ming-Jiang, SHI Qing-Fan, SUN Gang
- 054206 Wavelength Modulation Absorption Spectroscopy Using a Frequency-Quadruped Current-Modulated System**  
SHAO Jie, SUN Hui-Juan, WANG Hui, ZHOU Wei-Dong, WU Gen-Zhu



- 054207 Intensity Spatial Profile Analysis of a Gaussian Laser Beam at Its Waist Using an Optical Fiber System**  
ZHANG Liangmin
- 054208 Silicon-Based Asymmetric Add-Drop Microring Resonators with Ultra-Large Through-Port Extinctions**  
XIAO Xi, LI Yun-Tao, YU Yu-De, YU Jin-Zhong
- 054209 Measurement of Ultrashort Laser Pulse Width in a Wide Spectrum Range Using Dimethyl Sulfoxide by Optical Kerr Effect Technique**  
KONG De-Gui, CHANG Qing, YE Hong-An, GAO Ya-Chen, ZHANG Li-Xin, WANG Yu-Xiao, ZHANG Xue-Ru, YANG Kun, SONG Ying-Lin
- 054210 Synthesis of Fiber Bragg Gratings with Right-Angled Triangular Spectrum**  
LI Li-Sha, FENG Xuan-Qi
- 054211 Generation of Sub-2 Cycle Optical Pulses with a Differentially Pumped Hollow Fiber**  
ZHANG Wei, TENG Hao, YUN Chen-Xia, ZHONG Xin, HOU Xun, WEI Zhi-Yi
- 054212 Residual Doppler Effect on Electromagnetically Induced Transparency in a Zeeman Sublevel System**  
HU Zhen-Yan, LI Lu-Ming, CHEN Pei-Rong, SUN Xin
- 054213 Suppercontinuum Generation in InP Nano Inner Cladding Fibers**  
DUAN Yu-Wen, ZHANG Ru, WANG Jin, CHEN Xi, ZHONG Kun
- 054301 A Combined Reconstruction Algorithm for Limited-View Multi-Element Photoacoustic Imaging**  
YANG Di-Wu, XING Da, ZHAO Xue-Hui, PAN Chang-Ning, FANG Jian-Shu
- 054701 Capillary Rise in a Single Tortuous Capillary**  
CAI Jian-Chao, YU Bo-Ming, MEI Mao-Fei, LUO Liang
- 054702 Intermittency and Thermalization in Turbulence**  
ZHU Jian-Zhou, Mark Taylor
- 054703 Generation Mechanism of Liquid Column during the Burst of a Rising Bubble near a Free Surface**  
WANG Han, ZHANG Zhen-Yu, YANG Yong-Ming, ZHANG Hui-Sheng
- PHYSICS OF GASES, PLASMAS, AND ELECTRIC DISCHARGES**
- 055201 Electron Emission Suppression from Cathode Surfaces of a Rod-Pinch Diode**  
GAO Yi, YIN Jia-Hui, SUN Jian-Feng, ZHANG Zhong, ZHANG Peng-Fei, SU Zhao-Feng
- 055202 First Charge Exchange Recombination Spectroscopy Diagnostic in HL-2A Tokamak**  
HAN Xiao-Yu, DUAN Xu-Ru, YANG Li-Mei, YU De-Liang, ZHONG Wu-Lv, FU Bing-Zhong, LIU Yong, LIU Yi, YAN Long-Wen, YANG Qing-Wei
- 055203 Characteristics of a Novel Water Plasma Torch**  
NI Guo-Hua, MENG Yue-Dong, CHENG Cheng, LAN Yan
- 055204 Propagation Characteristics of Whistler-Mode Chorus during Geomagnetic Activities**  
ZHOU Qing-Hua, HE Yi-Hua, HE Zhao-Guo, YANG Chang
- CONDENSED MATTER: STRUCTURE, MECHANICAL AND THERMAL PROPERTIES**
- 056101 Quantitative Characterization of Partial Dislocations in Nanocrystalline Metals**  
NI Hai-Tao, ZHANG Xi-Yan, ZHU Yu-Tao
- 056201 Frequency Response of Sample Vibration Mode in Scanning Probe Acoustic Microscope**  
ZHAO Ya-Jun, CHENG Qian, QIAN Meng-Lu
- 056801 Temperature-Dependent Raman Spectrum of Hexagonal YMnO<sub>3</sub> Films Synthesized by Chemical Solution Method**  
LIU Yue-Feng, WANG Bei, ZHENG Hai-Wu, LIU Xiang-Yang, GU Yu-Zong, ZHANG Wei-Feng



- 056802 Influence of Au-Doping on Morphology and Visible-Light Reflectivity of TiN Thin Films Deposited by Direct-Current Reactive Magnetron Sputtering**  
NA Yuan-Yuan, WANG Cong, LIU Yu
- 056803 Research of Equilibrium Composition Map in Conic Quantum Dots**  
ZHAO Wei, YU Zhong-Yuan, LIU Yu-Min, FENG Hao, XU Zi-Huan
- 056804 Large-Area Self-Assembly of Rubrene on Au(111) Surface**  
LIU Xiao-Qing, KONG Hui-Hui, CHEN Xiu, DU Xin-Li, CHEN Feng, LIU Nian-Hua, WANG Li
- CONDENSED MATTER: ELECTRONIC STRUCTURE, ELECTRICAL, MAGNETIC, AND OPTICAL PROPERTIES**
- 057101 Quantum Mechanical Study on Tunnelling and Ballistic Transport of Nanometer Si MOSFETs**  
DENG Hui-Xiong, JIANG Xiang-Wei, TANG Li-Ming
- 057102 Spectral Response and Photoelectrochemical Properties of  $\text{Cd}_{1-x}\text{Zn}_x\text{Se}$  Films**  
N. J. Suthan Kissinger, G. Gnana Kumar, K. Perumal, J. Suthagar
- 057103 Mechanism of Visible Photoactivity of F-Doped  $\text{TiO}_2$**   
GUO Mei-Li, ZHANG Xiao-Dong, LIANG Chun-Tian, JIA Guo-Zhi
- 057104 Variation of Optical Quenching of Photoconductivity with Resistivity in Unintentional Doped GaN**  
HOU Qi-Feng, WANG Xiao-Liang, XIAO Hong-Ling, WANG Cui-Mei, YANG Cui-Bai, LI Jin-Min
- 057201 Thermoelectric Performances of Free-Standing Polythiophene and Poly(3-Methylthiophene) Nanofilms**  
LU Bao-Yang, LIU Cong-Cong, LU Shan, XU Jing-Kun, JIANG Feng-Xing, LI Yu-Zhen, ZHANG Zhuo
- 057202 Spin Current Through Triple Quantum Dot in the Presence of Rashba Spin-Orbit Interaction**  
LI Jin-Liang, LI Yu-Xian
- 057301 Anomalous Effect of Interface Traps on Generation Current in Lightly Doped Drain nMOS-FET's**  
MA Xiao-Hua, GAO Hai-Xia, CAO Yan-Rong, CHEN Hai-Feng, HAO Yue
- 057302 Shape-Controlled Synthesis and Related Growth Mechanism of  $\text{Pb}(\text{OH})_2$  Nanorods by Solution-Phase Reaction**  
CHENG Jin, ZOU Xiao-Ping, SONG Wei-Li, CAO Mao-Sheng, SU Yi, YANG Gang-Qiang, LÜ Xue-Ming, ZHANG Fu-Xue
- 057303 Infrared Absorption Spectra of Undoped and Doped Few-Layer Graphenes**  
XU Yue-Hua, JIA Yong-Lei, ZHOU Jian, DONG Jin-Ming
- 057304 Observation of Coulomb Oscillations with Single Dot Characteristics in Heavy Doped Ultra Thin SOI Nanowires**  
FANG Zhong-Hui, ZHANG Xian-Gao, CHEN Kun-Ji, QIAN Xin-Ye, XU Jun, HUANG Xin-Fan, HE Fei
- 057305 Blue Luminescent Properties of Silicon Nanowires Grown by Solid-Liquid-Solid Method**  
PENG Ying-Cai, FAN Zhi-Dong, BAI Zhen-Hua, ZHAO Xin-Wei, LOU Jian-Zhong, CHENG Xu
- 057306 White Emitting ZnS Nanocrystals: Synthesis and Spectrum Characterization**  
HUANG Qing-Song, DONG Dong-Qing, XU Jian-Ping, ZHANG Xiao-Song, ZHANG Hong-Min, LI Lan
- 057501 Microwave Magnetic Properties and Natural Resonance of  $\epsilon$ -Co Nanoparticles**  
YANG Yong, XU Cai-Ling, QIAO Liang, Li Xing-Hua, LI Fa-Shen
- 057502 Effective Anisotropy in Magnetically  $\text{Nd}_2\text{Fe}_{14}\text{B}/\alpha\text{-Fe}$  Nanocomposite**  
GUO Jia-Jun, CHEN Lei, ZHAO Xu, FAN Su-Li, CHEN Wei
- CROSS-DISCIPLINARY PHYSICS AND RELATED AREAS OF SCIENCE AND TECHNOLOGY**
- 058101 Improvement of AlN Film Quality by Controlling the Coalescence of Nucleation Islands in Plasma-Assisted Molecular Beam Epitaxy**  
ZHANG Chen, HAO Zhi-Biao, REN Fan, HU Jian-Nan, LUO Yi

- 058102 Preparation of Functional Gradient Material n-PbTe with Continuous Carrier Concentration**  
ZHU Pin-Wen, HONG You-Liang, WANG Xin, CHEN Li-Xue, IMAI Yoshio
- 058103 Deposition Behavior and Mechanism of Ni Nanoparticles on Surface of SiC Particles in Solution Systems**  
XU Hui, KANG Yu-Qing, ZHANG Lu, JIN Hai-Bo, WEN Bo, WEN Bao-Li, YUAN Jie, CAO Mao-Sheng
- 058501 A Single Photon Counting Detector Based on One-Dimensional Vernier Anode**  
YANG Hao, ZHAO Bao-Sheng, SHENG Li-Zhi, LI Mei, YAN Qiu-Rong, LIU Yong-An
- 058502 Extrinsic Base Surface Passivation in High Speed “Type-II” GaAsSb/InP DHBTs Using an InGaAsP Ledge Structure**  
LIU Hong-Gang, JIN Zhi, SU Yong-Bo, WANG Xian-Tai, CHANG Hu-Dong, ZHOU Lei, LIU Xin-Yu, WU De-Xin
- 058901 Detecting Overlapping Communities Based on Community Cores in Complex Networks**  
SHANG Ming-Sheng, CHEN Duan-Bing, ZHOU Tao
- 058902 Increase of Traffic Flux in Two-Route Systems by Disobeying the Provided Information**  
SUN Xiao-Yan, JIANG Rui, WANG Bing-Hong

#### **GEOFYSICS, ASTRONOMY, AND ASTROPHYSICS**

- 059101 Prediction and Elimination of Multiples Based on Energy Flux Conservation Theorem and Prediction Operator Equation**  
He Li, LIU Hong, DING Ren-Wei, LI Bo

JUST FOR AUTHORS  
— CHINESE PHYSICS LETTERS